Dexrazoxane Abrogates Acute Doxorubicin Toxicity in Marmoset Ovary 1

Authors: Salih, Sana M., Ringelstetter, Ashley K., Elsarrag, Mazin Z., Abbott, David H., and Roti, Elon C. Roti

Source: Biology of Reproduction, 92(3)

Published By: Society for the Study of Reproduction

URL: https://doi.org/10.1095/biolreprod.114.119495

BIOLOGY OF REPRODUCTION (2015) **92**(3):73, 1–11
Published online before print 21 January 2015.
DOI 10.1095/biolreprod.114.119495

Dexrazoxane Abrogates Acute Doxorubicin Toxicity in Marmoset Ovary[1]

Sana M. Salih,[2,4] Ashley K. Ringelstetter,[4] Mazin Z. Elsarrag,[4] David H. Abbott,[4,5] and Elon C. Roti Roti[3,4]

[4]*Department of Obstetrics and Gynecology, Divisions of Reproductive Endocrinology and Infertility and Reproductive Sciences, University of Wisconsin, Madison, Wisconsin*
[5]*Wisconsin National Primate Research Center, University of Wisconsin, Madison, Wisconsin*

ABSTRACT

Preservation of ovarian function following chemotherapy for nonovarian cancers is a formidable challenge. For prepubescent girls, the only option to prevent chemotherapy damage to the ovary is ovarian tissue cryopreservation, an experimental procedure requiring invasive surgeries to harvest and reimplant tissue, which carries the risk of cancer reintroduction. Drugs that block the primary mechanism of chemotherapy insult, such as dexrazoxane (Dexra) in the context of anthracycline chemotherapy, provide a novel approach for ovarian protection and have the potential to overcome current limitations to oncofertility treatment. Dexra is a catalytic topoisomerase 2 inhibitor that protects the mouse ovary from acute doxorubicin (DXR) chemotherapy toxicity in vitro by preventing DXR-induced DNA damage and subsequent gammaH2AX activation. To translate acute DXR ovarian insult and Dexra protection from mouse to nonhuman primate, freshly obtained marmoset ovarian tissue was cultured in vitro and treated with vehicle or 20 μM Dexra 1 h prior to 50 nM DXR. Cultured ovarian tissue was harvested at 2, 4, or 24 h post-DXR treatment. Dexra prevented DXR-induced DNA double-strand breaks as quantified by the neutral comet assay. DXR treatment for 24 h increased gammaH2AX phosphorylation, specifically increasing the number of foci-positive granulosa cells in antral follicles, while Dexra pretreatment inhibited DXR-induced gammaH2AX phosphorylation foci formation. Additionally, Dexra pretreatment trended toward attenuating DXR-induced AKT1 phosphorylation and caspase-9 activation as assayed by Western blots of ovarian tissue lysates. The combined findings suggest Dexra prevents primary DXR-induced DNA damage, the subsequent cellular response to DNA damage, and may diminish early apoptotic signaling in marmoset ovarian tissue. This study provides initial translation of Dexra protection against acute ovarian DXR toxicity from mice to marmoset monkey tissue.

cancer survivor, dexrazoxane, doxorubicin, fertility, marmoset, ovary

INTRODUCTION

Girls and women who survive cancer are at increased risk for primary ovarian insufficiency leading to failure of pubertal development and infertility [1–4]. Prepubescent girls are particularly vulnerable because they are not suitable candidates for current clinically approved fertility preservation options, including embryo and oocyte cryopreservation [5]. While ovarian tissue cryopreservation is available for children, it is still considered experimental and carries the risk of causing cancer relapse via the requisite tissue autotransplantation [6–12]. A drug-based ovarian shield given routinely at the time of chemotherapy treatment may preserve both fertility and ovarian estrogen regulation in young children, adolescents, and adult female cancer survivors, thus overcoming current obstacles in oncofertility. Putative ovarian protective (ovoprotective) drugs have the potential to provide timely, effective, noninvasive, easy-to-administer, and affordable prophylactics to preserve ovarian follicular and endocrine function. Tested as a putative ovoprotective drug, gonadotropin-releasing hormone (GnRH) agonists, which indirectly suppress ovarian function by inhibiting release of gonadotropins from pituitary gonadotropes, have been tested for their ability to act as ovoprotective agents and preserve fertility in female cancer patients [13, 14]. While effective in controlling menstrual cyclicity during chemotherapy, GnRH agonists have had mixed results in clinical trials of fertility preservation in cancer patients [12, 15]. While a previous study elegantly demonstrated that apoptotic inhibitors attenuate cell death in response to radiation in the nonhuman primate ovary [16], only a handful of other drugs have been suggested as candidates for ovoprotection from chemotherapy, with dexrazoxane (Dexra) and bortezomib providing the only mechanism-targeted approaches [16–27]. The current study provides a drug-based mechanism to prevent the primary mode of chemotherapy insult prior to the onset of apoptosis in nonhuman primate ovarian tissue.

Doxorubicin (DXR) is one of the most commonly utilized chemotherapy drugs and is routinely administered to treat tumors occurring in premenopausal females, including breast and childhood cancers [28, 29]. We and others have described DXR toxicity in the mouse ovary [20, 30–33]. DXR induces acute DNA damage and subsequent cellular and follicular demise in a complex manner involving temporal and spatial responses that are cell- and follicle-type specific [20]. A single dose of DXR is sufficient to induce DNA damage in mice, as manifested by increased DNA double-strand breaks (DSBs) in

[1]This work was supported by the University of Wisconsin Start-Up and Research and Development funds (MSN132883), Wisconsin Alumni Research Foundation (MSN162253), and NIH training grant K12 HD0558941 to S.M.S.; and by University of Wisconsin Cancer Center Support Grant P30CA014520. This publication was supported in part by the Office of the Director, National Institutes of Health under Award Number P51OD011106 to the Wisconsin National Primate Research Center, University of Wisconsin-Madison. This research was conducted in part at a facility constructed with support from Research Facilities Improvement Program grant numbers RR15459-01 and RR020141-01. The content is solely the responsibility of the authors and does not necessarily represent the official views of the National Institutes of Health.
[2]Correspondence: Sana M. Salih, Department of Obstetrics and Gynecology, 600 Highland Avenue, Clinical Science Center, H4/626, University of Wisconsin, Madison, WI 53792. E-mail: sanasalih5@gmail.com
[3]Current address: Department of Medicine, University of Wisconsin, Madison, WI 53792.

Received: 29 April 2014.
First decision: 8 May 2014.
Accepted: 30 December 2014.

eISSN: 1529-7268 http://www.biolreprod.org
ISSN: 0006-3363

stromal/thecal cells as early as 2 h postinjection, followed by DNA damage in granulosa cells and later, oocytes [20]. In the ovaries of treated mice, γH2AX activation is measurable at 6 h post-DXR, with increased apoptosis in granulosa cells of growing follicles measurable by 8–10 h post-DXR-treatment [20]. Our mouse study thus defines a narrow 2-h window of opportunity to prevent DXR toxicity with novel medicinal therapy prior to the onset of somatic cell DNA damage. The current study investigates the ability of the cardio- and skin-protectant drug Dexra to shield the marmoset ovary from acute DXR ovarian insult [34–36]. Pretreatment with Dexra, a catalytic topoisomerase II inhibitor and antioxidant, attenuates DXR-induced DNA DSBs, increases ovarian cell viability, and inhibits DXR-induced γH2AX activation in cultured mouse ovaries [34]. The ability to prevent DXR-induced DNA DSBs established Dexra as the first mechanistic ovarian shield against chemotherapy toxicity [34]. With proven efficacy to protect against DXR-induced cardiomyopathy and skin extravasation without limiting DXR toxicity within cancer cells [35–38] and the ability to shield both dividing and quiescent cells, Dexra is an ideal drug to protect the ovary, which contains mixed cell populations at varying stages of cycle and quiescence.

While we have described ovarian protection from DXR insult in mouse tissue [27, 34], such studies do not always faithfully translate to humans [39]. Nonhuman primates, including marmoset monkeys, constitute a translational model that may more closely replicate both DXR ovarian insult and protection in humans [40, 41]. Marmosets are valuable nonhuman primates in which to model ovarian toxicity and fertility preservation, with a relatively short generation time (adult by ~1.5–2 yr of age) and gestation length (5 mo) [42–44]. Comparable to humans, marmoset folliculogenesis is characterized by the development of dominant preovulatory follicles under the influence of follicle-stimulating hormone (FSH) [45]. Considering species similarities between nonhuman primate and human ovaries, it is essential to assess chemotherapy toxicity and protection in a nonhuman primate prior to pioneering Dexra for drug-based fertility preservation studies in humans [39]. The current study presents an initial study demonstrating Dexra protection against DXR toxicity using an in vitro marmoset ovarian tissue culture system.

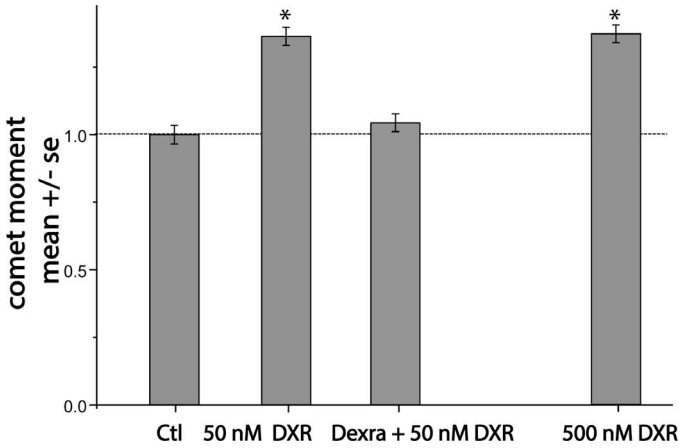

FIG. 1. Pretreatment with Dexra prevents DXR-induced DNA damage in marmoset ovarian cells. NCA summary data indicate pretreatment with Dexra prevented an acute DXR-induced increase in DNA DSBs in pooled ovarian cells in marmoset ovarian tissue at 4 h post-DXR treatment. For each individual experiment, the increases in DNA DSBs caused by both doses of DXR exceeded control values, while Dexra pretreatment was similar to control baseline. In vitro cultured marmoset ovarian tissue slices were pretreated with vehicle for 1 h followed by 50 or 500 nM DXR or with 20 μM Dexra for 1 h followed by 50 nM DXR treatment. Ovarian tissue slices were harvested at 4 h post-DXR treatment. DNA damage was quantified in pooled somatic ovarian cells as the Olive moment, summarized in a bar graph of data pooled from three experiments (n = 3 marmosets; each experimental sample was run in duplicate, >100 somatic cells per data collection point, $^*P < 0.05$, one-way ANOVA).

MATERIALS AND METHODS

Chemicals and Drugs

DXR was provided as DXR hydrochloride in a 2 mg/ml aqueous solution (Teva Parenteral Medicines). Dexra was provided as powdered Dexra hydrochloride (Zinecard; Pharmacia & Upjohn Company). Dexra was solubilized as 80 mM in 0.167 M sodium lactate immediately before use and diluted to a final 20 μM concentration in the culture media.

Animals

No live animal work was conducted in the current study. Marmoset ovaries harvested at the Wisconsin National Primate Research Centers (WNPRC) were obtained through the WNPRC's Nonhuman Biological Material Distribution Core. Fresh marmoset ovaries were collected under general anesthesia in conjunction with independent studies. The WNPRC coprincipal investigators of the studies that harvested the monkey ovaries (J. E. Levine and D. H. Abbott) gave permission for the authors to use those ovaries for this study. The care, housing, and harvesting of tissues from female marmoset monkeys (*Callithrix jacchus*) at WNPRC were fully compliant with the recommendations of the Guide for the Care and Use of Laboratory Animals and the Animal Welfare Act. The Institutional Animal Care and Use Committees and Graduate School, University of Wisconsin, Madison, approved all the procedures prior to implementation.

Marmoset ovaries from 10 multiparous/nulliparous adult female common marmosets, median age ~3.5 yr, were obtained either under general anesthesia (1%–5% isoflurane/oxygen) or following premedication with ketamine (at least 15 mg/kg injected intramuscularly) and induction of a deep plane of anesthesia with an intravenous injection of sodium pentobarbital (25–50 mg/kg) to effect stoppage of the heart, permitting necropsy. The harvested ovaries enabled development of an in vitro marmoset ovarian tissue culture system to assess DXR toxicity and Dexra protection from acute DXR insult. Ovaries were placed in 5 ml of sterile PBS, and cleansed of any attached tissue. One ovary from each animal was used for this study and was sliced with the Stadie Riggs Tissue Slicer (Thomas Scientific). Ovarian tissue slices cut along the longitudinal axis of each ovary were cut into eight wedges, and each wedge was transferred randomly to a filter basket (Millipore) in a well containing ovary culture media described previously (Ham F12/DMEM phenol red, 1 mg/ml bovine serum albumin (BSA), 1 mg/ml Albumax, 0.05 mg/ml ascorbic acid, 5 units/ml penicillin 5 μg/ml streptomycin, and 0.0275 mg/ml transferrin) [34]. Four treatment groups were used for all experiments: 1) vehicle control for Dexra (0.167 M sodium lactate) + vehicle control for DXR (PBS, pH 7.4), 2) vehicle control for Dexra + 50 nM DXR, 3) vehicle control for Dexra + 500 nM DXR, and 4) 20 μM Dexra + 50 nM DXR. Although Dexra pretreatment was performed in conjunction with 50 nM DXR, this was not done in conjunction with 500 nM DXR because of limited tissue availability. Cotreatment using 50 nM DXR was chosen because that concentration was sufficient to cause a toxicity response, and 500 nM is outside the upper range of circulating DXR concentrations in patients receiving chemotherapy. Ovarian tissues from three to four animals were used for each endpoint assay: neutral comet assay (NCA), Western blot analysis, or immunofluorescence. Ovarian tissue slices were treated with Dexra or vehicle control for 1 h prior to the addition of DXR to the culture media. DXR and Dexra were continuously present in the culture media for the entire culture duration. Tissues were harvested for assays at 2, 4, and/or 24 h after the addition of DXR to the culture media. Small pieces of tissue were processed for the NCA to quantify DXR-induced DNA DSBs and the remaining ovarian tissue slices were used to extract protein or fixed in 4% formalin [20, 34].

NCA

Cells were isolated from marmoset ovarian slices to create a single cell suspension at 2 and 4 h post-DXR treatment. Slices were further chopped in a solution of 0.25% collagenase/PBS, pH 7.4, and incubated for 30 min total at 37°C. Every 15 min during that incubation, tissues were passed six times through a 23-gauge needle to disperse the cells. Cells were centrifuged for 10 min at 300 × *g* to pellet. Collagenase-containing solution was removed, and

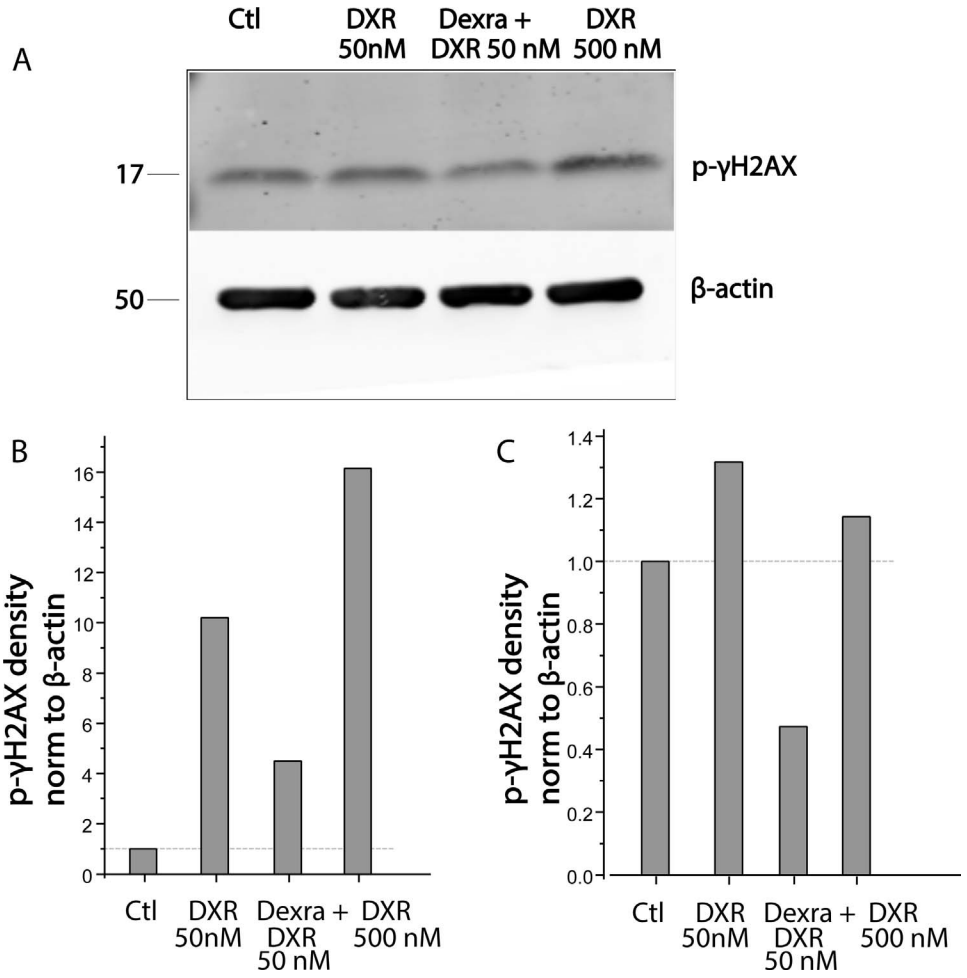

FIG. 2. Dexra pretreatment attenuates DXR-induced H2AX phosphorylation in marmoset ovarian tissue protein lysates. Marmoset ovarian tissue culture slices were pretreated with vehicle control (Ctl) for 1 h followed by 50 or 500 nM DXR or with 20 μM Dexra 1 h followed by 50 nM DXR treatment. Cultured ovarian tissue slices from four marmosets were harvested at 4 h post-DXR treatment. **A**) Representative Western blots from one animal probed with antibodies against phospho-γH2AX and β-actin (loading control) as indicated. **B** and **C**) Summary bar graphs of γH2AX phosphorylation from two individual marmoset animals exhibiting increased γH2AX phosphorylation at 4 h after 50 nM DXR (n = 4). Dexra significantly decreased DXR-induced γH2AX phosphorylation in one animal (**B**) and diminished the levels of p-γH2AX phosphorylation below control in the second animal (**C**).

each pellet was resuspended in 100 μl of 1 mg/ml proteinase K in PBS and incubated 5 min at room temperature (RT). At this point, the samples were blinded, resuspended in 350 μl 1% low melting agarose/PBS, plated on slides, and processed for the NCA as previously described [20, 34]. Stromal, thecal, and granulosa cells were analyzed together without distinction (no separation of different cell types) because of the small sample size. Images were collected on an Olympus microscope using a 20× objective and SPOT Plus software. At least 100 somatic cells per time point, per treatment group, per animal were imaged. Olive moment quantification of DNA DSBs was scored using CometScore software (TriTek Corporation) [20, 34].

Protein Lysate Preparation and Western Blot Analysis

Whole-cell protein lysates were prepared from cultured marmoset ovarian tissue homogenized in RIPA buffer that included phosphatase inhibitors and complete protease inhibitors (Roche/Life Technologies). Protein quantification was determined using the Bio-Rad DC Protein Assay per the manufacturer's instructions (Bio-Rad). Protein lysates were heated for 5 min at 75°C in 1× Laemmli sample buffer prior to loading 10 or 20 μg total protein per lane, and the samples were separated by size on 4%–20% SDS-PAGE gradient gels (Bio-Rad) under reducing conditions. Proteins were transferred to polyvinylidene fluoride-Fl (Millipore), and the membranes were preblocked in TBS-T (20 mM Tris Base, 137 mM NaCl, 1 M HCl) + 5% BSA (for phospho-specific antibodies) or + 5% milk for 1 h at RT. Western blots were probed with rabbit anti-S139-phosphorylated γH2AX (1:500; Abcam), rabbit anti-caspase-9 (1:1000; Cell Signaling), rabbit anti-S473-phosphorylated (activated) pAKT1 (1:1000; Cell Signaling), rabbit anti-PTEN (phosphatase and tensin homolog) (1:1000; Cell Signaling), or mouse-anti-β actin (1:10 000; Sigma) in TBS-T + 5% BSA or milk overnight at 4°C. Blots were washed with TBS-T then probed simultaneously with secondary antibodies, donkey anti-rabbit Alexa 680 (Molecular Probes) and donkey anti-mouse IRdye 800 (LiCor), both at 1:15 000 in TBS-T for 1 h at RT. Western blots were washed with TBS-T, dried, and scanned using the LiCor Odyssey System (University of Wisconsin-Small Molecule Screening Facility). Density measurements were taken using the Odyssey software.

Phospho-γH2AX Immunostaining

Phospho-γH2AX protein expression was detected in 5 μm ovarian tissue sections as previously described [20]. Tissue sections were deparaffinized, hydrated through graded ethanol, and rinsed for 5 min in distilled-deionized H_2O. Sections were blocked for 1 h at RT using 10% goat serum in PBS followed by a PBS wash. Sections were then incubated with rabbit anti-phospho-γH2AX (Cell Signaling) at a 1:480 dilution in PBS with 1% goat serum overnight at 4°C. Sections were rinsed three times for 5 min in PBS. Secondary staining was performed with goat anti-rabbit Alexa Fluor 488 (Invitrogen) at a 1:400 dilution in PBS for 30 min at RT in the dark. Slides were rinsed three times for 5 min each in PBS. Slides were mounted with ProLong Gold antifade reagent containing 4′,6-diamidino-2-phenylindole (DAPI) (Invitrogen) to counterstain nuclei, and the coverslips were placed. Slides were imaged on the Nikon A1 confocal laser microscope (three ovaries/treatment type).

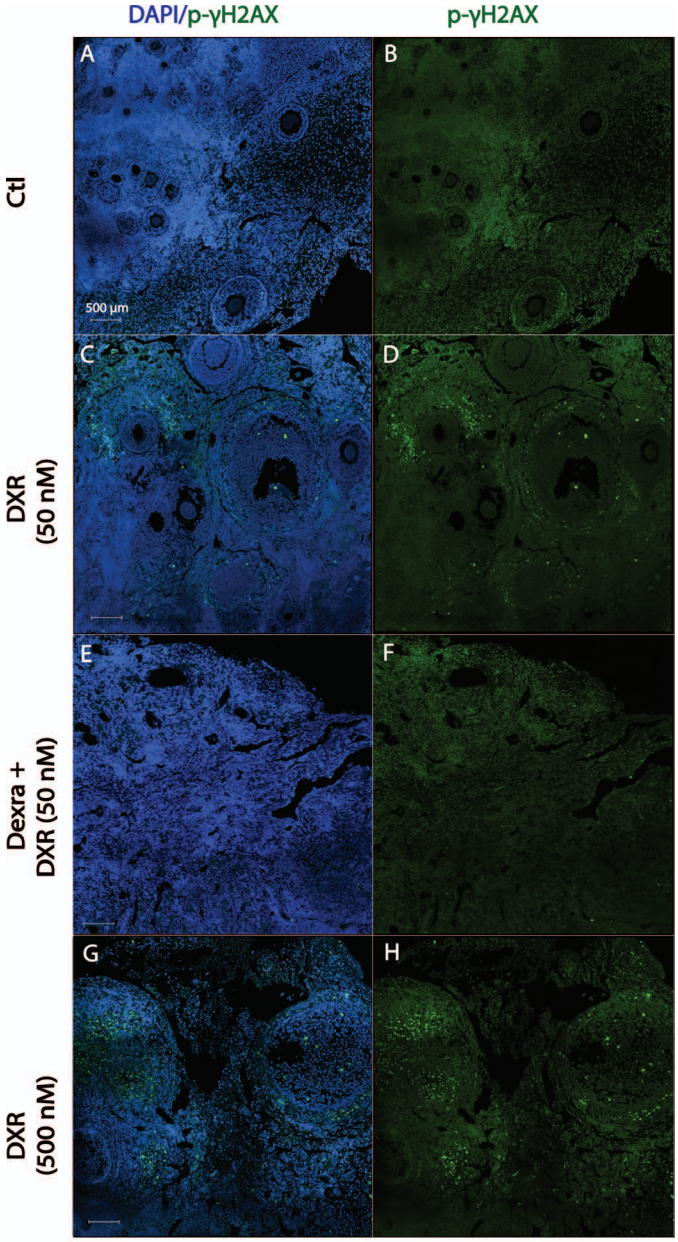

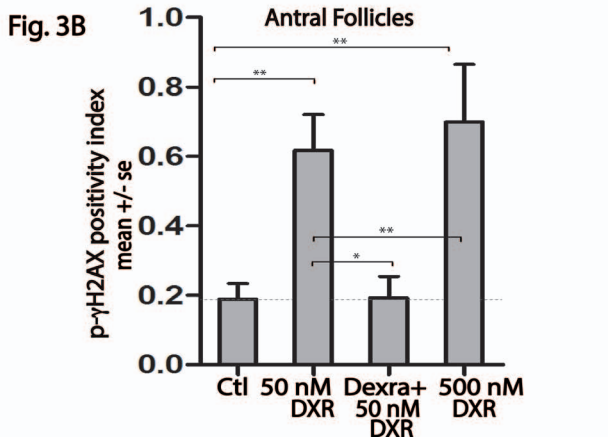

FIG. 3. Dexra pretreatment decreases the number of follicles containing phospho-γH2AX foci-positive granulosa cells. Marmoset ovarian tissue culture slices were treated with vehicle control or DXR ± Dexra and fixed at 24 h post-DXR treatment. Ovarian sections were stained for p-γH2AX (green) and nuclei (blue, DAPI). **A**) Representative fluorescent images (**A**–**H**) demonstrate formation of p-γH2AX foci in marmoset ovarian sections for each treatment condition from the same animal (**A** and **B** = control, **C** and **D** = 50 nM DXR, **E** and **F** = Dexra + 50 nM DXR, **G** and **H** = 500 nM DXR). Bar = 500 µm for all the images. **B**) Summary bar graphs of p-γH2AX-positive antral follicles at 24 h after 50 and 500 nM DXR treatment ± Dexra. A growing follicle is considered positive if it contains at least four p-γH2AX-positive granulosa cells per follicle; $^{*}P < 0.05$ and $^{**}P < 0.001$, one-way ANOVA, Bonferroni means comparison (n = 3 animals).

Fluorescence Microscopy for Detection of Phospho-γH2AX Staining

Images for p-γH2AX-stained slides were collected using a Nikon A1 laser-scanning confocal microscope (WNPRC for Biological Imaging). Alexa Fluor 488 fluorescein isothiocyanate (p-γH2AX-positive cells) was detected at an excitation wavelength of 488 nm and emission wavelength of 525 nm. To detect DAPI, the excitation was at 403.6 nm and the emission was collected at 450–465 nM. Laser settings were determined by imaging control samples and setting laser intensities to minimize autofluorescence. Laser settings were then held constant for all the experimental samples. Each image was taken at the Z plane providing maximal signal in the given section. Merged and individual channels were collected under simultaneous excitation. Follicle types were identified using standard morphology and size ranges from parallel-stained hematoxylin and eosin slides [46]. Phospho-γH2AX-positive granulosa or stroma cells had green nuclear staining. A predefined cutoff level to label an entire follicle as p-γH2AX positive was used based on previously reported TdT-mediated dUTP nick end labeling assay and follicle atresia studies [20, 46]; all the follicles were considered positive if they had at least four p-γH2AX-positive granulosa cells except for primordial follicles, which were considered positive with greater than or equal to one p-γH2AX-positive granulosa cell. The mean p-γH2AX-positivity index was calculated as the (number of p-γH2AX-positive follicles)/(total follicle count) for each follicle type based on 2–3 sections/ovary/treatment type.

Statistics

All the experiments were performed in triplicate for each treatment group. Graphs and statistical analyses were generated using OriginLab. One-way ANOVAs were conducted with Bonferroni tests for means comparisons (mean ± SEM). Data were normalized to the controls to allow pooling across experiments and were presented as fractional change compared to the controls. Differences were considered significant at $P < 0.05$. For follicle counts, ovarian tissue slices from the same animal were treated at the same time, and each tissue slice was analyzed as an independent sample.

RESULTS

Dexra Protects Marmoset Ovarian Tissue from DXR-Induced DNA Damage

To test the hypothesis that in vitro administration of Dexra protects marmoset ovarian tissue from DXR-induced DNA damage, cultured marmoset ovarian slices were pretreated with vehicle control for 1 h, followed by the addition of 50 or 500 nM DXR, or with 20 µM Dexra 1 h prior to the addition of 50 nM DXR. NCA showed no increase in DNA DSBs in treated cells at 2 h post-DXR addition (data not shown). By 4 h post-DXR, however, both 50 nM and 500 nM DXR, which span the 100–400 nM range of DXR serum blood concentration in humans [47], increased DNA DSBs by 36% and 37%, respectively, compared to the control (n = 3, $P < 0.05$; Figure 1). Dexra pretreatment prevented DNA damage induced by 50 nM DXR, maintaining DNA DSBs at control values (Fig. 1). These data demonstrate that Dexra shielded cultured marmoset ovarian tissue from early DXR-induced DNA damage.

Dexra Attenuates DXR-Induced Increase in γH2AX Phosphorylation in Marmoset Ovarian Tissue

Phosphorylation of γH2AX was assessed in lysates of marmoset ovarian tissue culture from four marmoset animals at

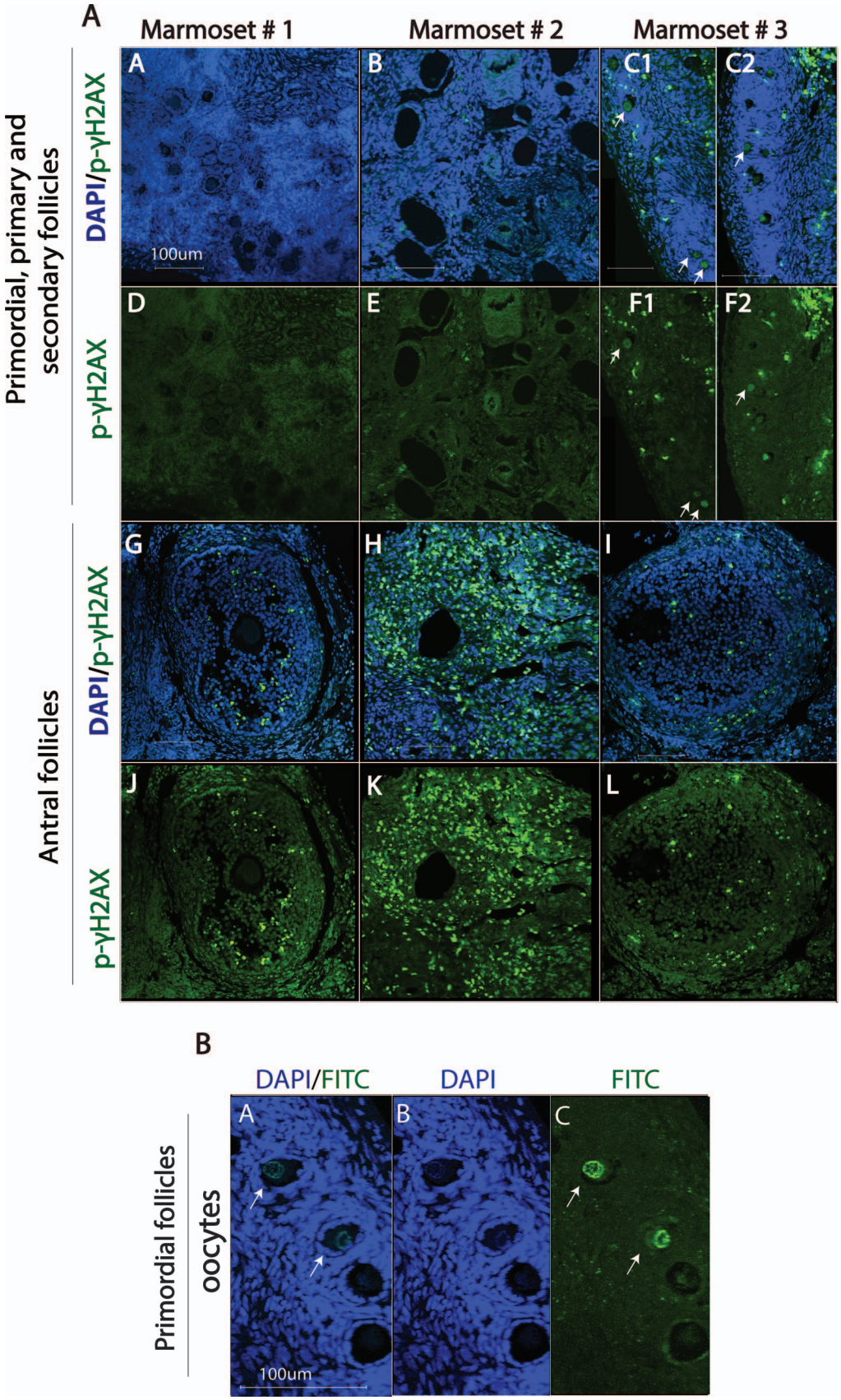

FIG. 4. DXR-induced formation of phospho-γH2AX foci in granulosa cells of antral follicles of marmoset ovarian tissue. Ovarian sections were stained for p-γH2AX (green) and nuclei (blue, DAPI). **A**) Representative fluorescent images (**A**–**L**) of marmoset ovarian sections from three different animals treated with 500 nM DXR are shown (**A**–**F** illustrate primordial, primary, and secondary follicles, **G**–**L** illustrate antral follicles). The arrows in **C** and **F** point to p-γH2AX-positive oocytes from primordial follicles. **B**) Digitally zoomed images show p-γH2AX-positive oocytes from primordial follicles (white arrows). Bar = 100 μm for all the images.

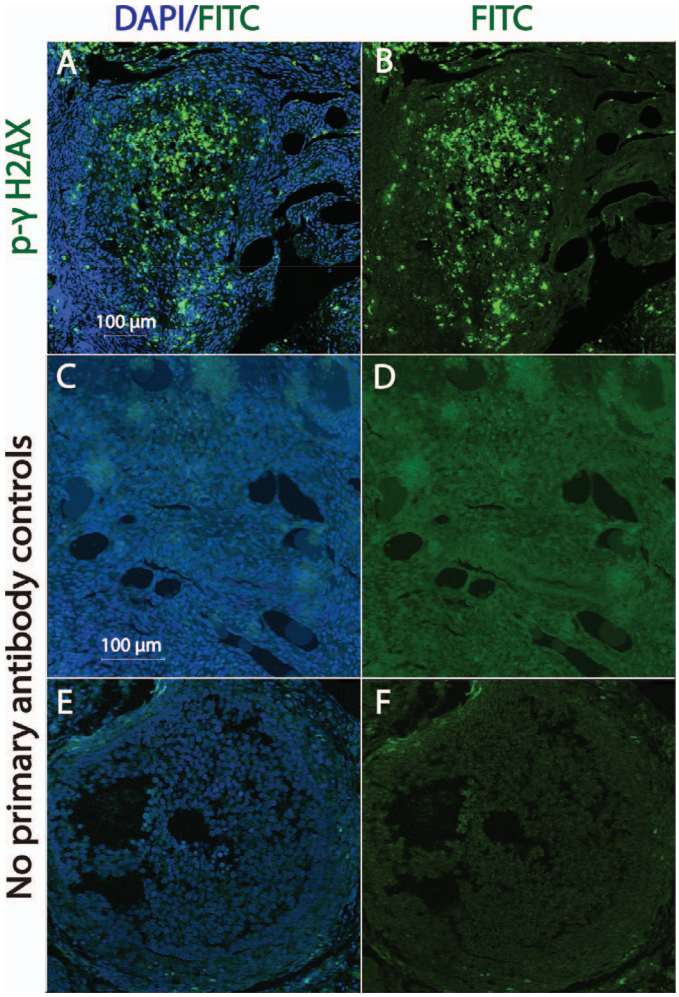

FIG. 5. DXR-induced formation of phospho-γH2AX foci within granulosa cells of corpus luteum of marmoset ovarian tissue. Ovarian sections were stained for p-γH2AX (green) and nuclei (blue, DAPI). Fluorescent images **A** and **B** illustrate corpus luteum exhibiting positive p-γH2AX staining. Photomicrographs **C** and **D** illustrate control ovarian tissue with no primary antibody added (no antral follicles seen). Photomicrographs **E** and **F** illustrate control ovarian tissue showing antral follicles with no primary antibody added. Bar = 100 μm.

4 h post-DXR addition to the culture media. Both 50 and 500 nM DXR increased the density of the band corresponding to phosphorylated γH2AX in two of the four animals at this time point. Dexra pretreatment protected ovarian tissue in the two animals that exhibited a DXR response at 4 h post-DXR treatment as demonstrated by phospho-γH2AX levels that were not different from the control on quantified Western blots. A representative Western blot probed with anti-phospho-γH2AX antibody at 4 h post-DXR treatment and individual bar graphs from the two responsive animals are shown in Figure 2.

Given the heterogeneous response at 4 h post-DXR, γH2AX phosphorylation was further assessed using immunofluorescence in marmoset ovarian tissue slice wedges that were harvested 24 h after treatment with DXR ± Dexra or vehicle control (n = 3 animals, 6–10 ovarian tissue slices per treatment). In contrast to the split phospho-γH2AX response at 4 h posttreatment, immunostaining at 24 h post-DXR revealed DXR increased the percentage of antral follicles containing p-γH2AX-positive granulosa cells in tissue from all animals when compared to vehicle control. In vehicle-treated tissue, 18.9% ± 4.4% of antral follicles were scored as phospho-γH2AX positive, with 50 and 500 nM DXR-treated tissue exhibiting 61.7% ± 10.3% ($P < 0.001$) and 69.9% ± 16.6% ($P < 0.001$) positive antral follicles, respectively (Fig. 3 and Supplemental Fig. S1, available online at www.biolreprod.org). Dexra pretreatment prevented the observed increase in γH2AX phosphorylation that occurred with 50 nM DXR treatment, maintaining the percentage of p-γH2AX-positive antral follicles at 19.2% ± 6.2% ($P < 0.05$), comparable to vehicle control (Fig. 3 and Supplemental Fig. S1). These data suggest that Dexra protects DXR-vulnerable antral follicles from chemotherapy insult, potentially delaying or diminishing loss of the growing follicle population. Contrary to antral follicles, γH2AX phosphorylation was observed with low frequency in granulosa cells of other preovulatory follicle types (primordial, primary, and secondary), often below the threshold of 1–4 positive cells/follicle at 24-h post-DXR treatment (Fig. 4). Interestingly, a handful of oocytes of primordial follicles exhibited γH2AX phosphorylation (~5%, Fig. 4) with 500 nM DXR treatment. Nuclear foci of phosphorylated γH2AX were noted in the highly vascularized corpora lutea (Fig. 5) [48], demonstrating the marked heterogeneity of γH2AX phosphorylation of different follicle types in cultured marmoset ovarian tissue.

Dexra Attenuates DXR-Induced Caspase-9 Cleavage in Marmoset Ovarian Tissue

To evaluate whether Dexra prevents acute DXR-induced apoptotic signaling, we quantified procaspase-9 cleavage as a marker for apoptosis. Quantification of the density of bands in Western blots corresponding to pro- and cleaved (activated) caspase-9 revealed that treatment with 50 or 500 nM DXR appeared to increase the ratio of cleaved to procaspase-9 at 24 h post-DXR treatment by 29% and 39%, ($P > 0.05$) over control, respectively (n = 3, Fig. 6). The cleaved to procaspase-9 ratio in tissue pretreated with Dexra prior to 50 nM DXR was not different from control-treated samples (<5% change), suggesting that Dexra attenuated the apparent trend in DXR-induced procaspase-9 cleavage at 50 nM, suggestive of a reduction in apoptosis.

Dexra Ameliorates DXR-Induced Changes in AKT1 Phosphorylation in Marmoset Ovarian Tissue

To investigate whether DXR insult affects mediators of cell survival and primordial follicle activation, we quantified phosphorylated AKT1 (v-akt murine thymoma viral oncogene homolog 1) and total PTEN protein expression at 2, 4, and 24 h post-DXR treatment. There were no changes in the density of the phosphorylated AKT1 band at 2 and 4 h post-DXR treatment (50 or 500 nM) on Western blots probed with anti-phospho AKT1 antibodies (not shown). There were trends toward a 25% ($P > 0.05$) increase in the density of phosphorylated pAKT1 on Western blots at 24 h after the addition of 50 nM DXR and ~45% increase ($P < 0.05$) following treatment with 500 nM DXR (n = 4; Fig. 7, A and B). Dexra prevented the upward trend in phosphorylated AKT1 following 50 nM DXR, producing levels similar to vehicle control (n = 4, $P > 0.05$; Fig. 7, A and B). These data suggest that Dexra may guard against the noted upward trend in DXR-induced perturbations in pAKT1, a cell survival and primordial follicle activation protein. PTEN protein expression was not affected by DXR because the corresponding band densities did not change with DXR treatment in marmoset ovarian tissue at

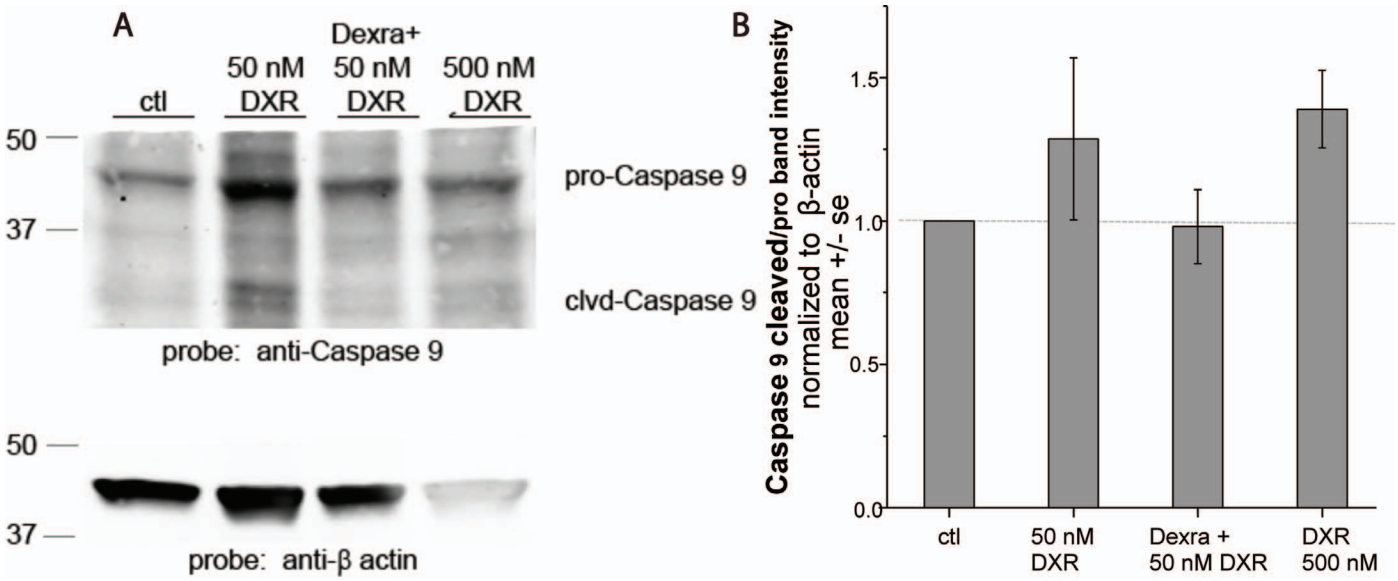

FIG. 6. Ratio of cleaved caspase-9 over total procaspase-9 levels in marmoset ovarian tissue tended to increase following DXR treatment, but not following DXR and Dexra pretreatment. Marmoset ovarian tissue culture slices were pretreated with vehicle control for 1 h followed by the addition of 50 or 500 nM DXR or with 20 μM Dexra 1 h prior to 50 nM DXR treatment. Ovaries were harvested 24 h post-DXR treatment (n = 3). **A**) Western blots probed with caspase-9 antibodies and β-actin as the loading control. **B**) Bar graph quantification of caspase-9 band density from ovarian tissue protein lysates. Lysates from ovarian tissue slices treated with DXR tended to exceed values for DXR with Dexra pretreatment or controls for ratios of cleaved caspase-9 over total procaspase-9 levels in marmoset ovarian tissue.

any tested time point (n = 4; Fig. 7, C and D, show 4 h post-DXR treatment while 2 and 24 h data not shown).

DISCUSSION

Girls who survive cancer are at increased risk for premature ovarian insufficiency due to chemotherapy toxicity. DXR chemotherapy induces ovarian damage leading to increased follicular demise and decreased fertility, with the extent of toxicity depending on the age of the patient and dose used [26, 49, 50]. We previously characterized DNA damage, subsequent γH2AX activation, and apoptosis in the mouse ovary over the acute insult period following DXR treatment [20]. Furthermore, we recently demonstrated that pretreatment with Dexra prevents DXR-induced ovarian toxicity in cultured mouse ovaries [34]. Prior to translation of drug-based ovarian protection to humans, it is important to validate efficacy and safety of putative ovoprotective drugs in a nonhuman primate model. The present study translates DXR acute insult and Dexra protection from mouse to a marmoset ovarian tissue culture model.

Dexra pretreatment prior to DXR prevented DXR-induced DNA damage in cultured marmoset ovarian tissue as measured by NCA at 4 h post-DXR, consistent with our previous in vitro mouse study [34]. To further examine the effect of Dexra on cellular responses to DNA damage in marmoset tissue, we quantified the levels of phosphorylated (activated) H2AX. Phosphorylation of H2AX is the earliest and most sensitive downstream cellular response to DNA damage [51] and typically parallels DNA DSBs [52]. The time line for γH2AX phosphorylation is species and tissue specific, however, and may vary depending on the type and dose of the offending agent [53, 54]. Only two out of four marmosets showed increased p-γH2AX band density in response to 4 h DXR treatment despite the fact that tissues from all the animals exhibited DXR-induced DNA damage at this time point. Dexra prevented the increase in γH2AX phosphorylation in the two responsive animals. Given that 4 h was the earliest time to detect DNA damage, γH2AX activation may have been more consistently detected if assayed at later time points. To corroborate the Western blot results, we assessed γH2AX phosphorylation by immunofluorescence at 24 h post-DXR treatment. Because there is no precedent for classifying entire follicles as p-γH2AX-positivite nor is the impact of γH2AX activation on follicle survival known, a scoring system was adopted from previous publications that used the TdT-mediated dUTP nick end labeling assay to score follicles as apoptotic [20, 46]. DXR treatment for 24 h increased p-γH2AX positivity in granulosa cells of antral follicles in all animals, suggesting that Western blots of tissue harvested at 4 h posttreatment may have contained samples that were collected at too premature a time to consistently detect γH2AX phosphorylation. Consistent with the Western blots of responsive animals, Dexra abrogated DXR-induced p-γH2AX phosphorylation in all animals at 24 h posttreatment. The immunofluorescence data importantly revealed striking heterogeneity of p-γH2AX immunostaining that was dependent upon follicle type and ovarian structure, with preferential γH2AX phosphorylation in granulosa cells of antral follicles and in the corpus luteum. The follicle- and corpus luteum-dependent activation of γH2AX would have contributed significantly to the mixed results of the Western blots because of the heterogeneity of the marmoset ovarian tissue slices. Future in vivo marmoset studies will determine the timing, pattern, and consequence of γH2AX activation in the follicular, stromal, and oocyte compartments of nonhuman primate ovaries.

Apoptosis occurs when cells fail to repair DNA damage despite recruitment of DNA repair proteins. When cell damage is severe and DNA repair insufficient, apoptosis-inducing downstream signaling effectors, including caspase-9, are activated, leading to cellular demise [55]. A marker of mitochondrial stress signaling and early apoptosis, procaspase-9 cleavage was quantified to determine whether Dexra

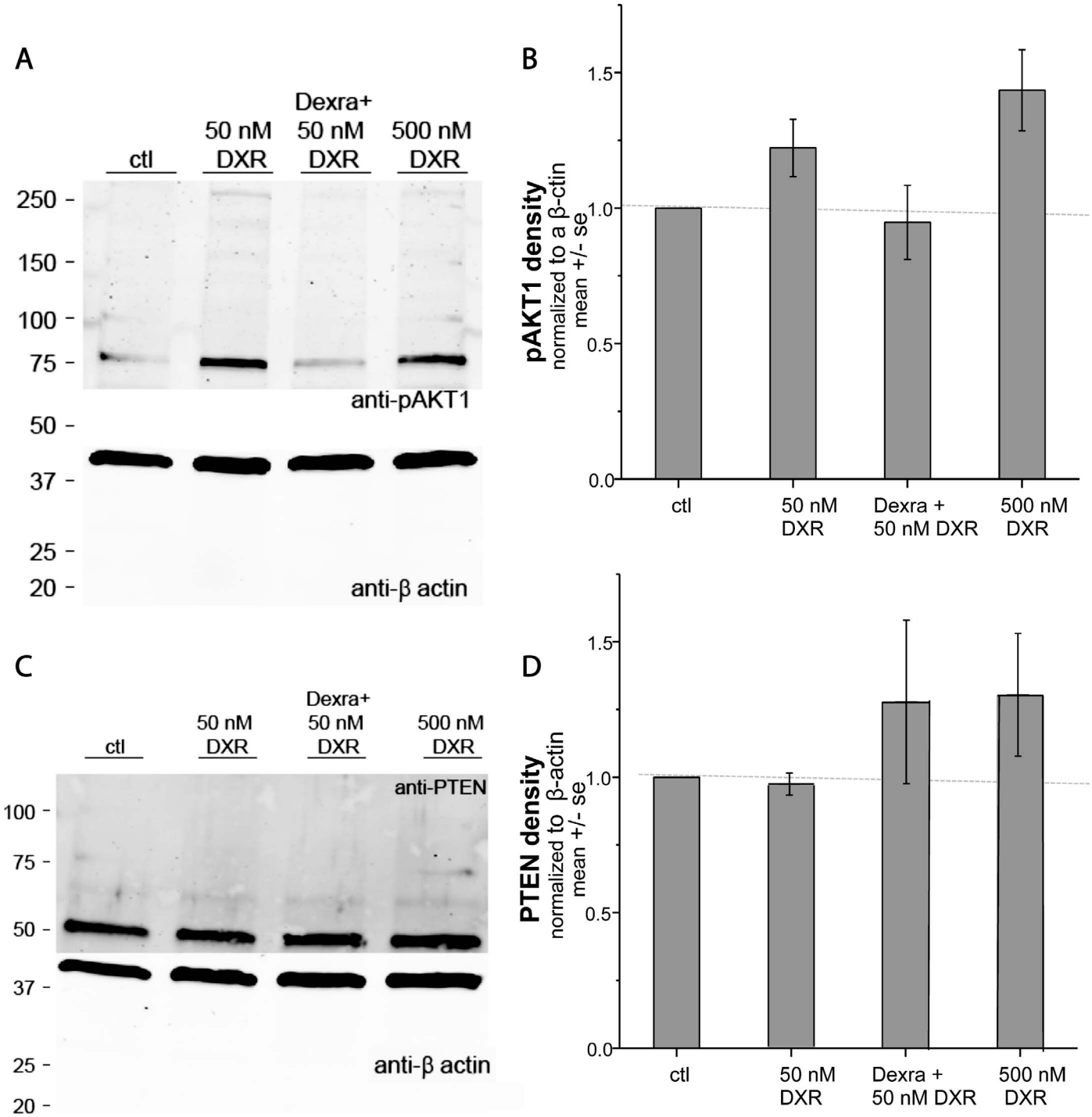

FIG. 7. AKT1 phosphorylation in marmoset ovarian tissue tended to increase following DXR treatment, but not following DXR and Dexra pretreatment. Western blot analysis of pAKT1 and PTEN proteins in marmoset ovarian tissue culture treated with vehicle control, DXR, or DXR ± Dexra. **A**) Western blot from one marmoset at 24 h post-DXR treatment probed with anti-pAKT1 and β-actin antibodies as indicated. **B**) Summary bar graph of Western blot data quantified from four marmosets at 24 h post-DXR treatment. DXR treatment tended to enhance induction of AKT1 phosphorylation at the 24-h time point, and this trend was obscured by Dexra pretreatment (n = 4). **C**) Example of Western blot of lysates of ovarian tissue harvested 4 h post-DXR probed with anti-PTEN and β-actin antibodies as indicated. **D**) Summary bar graph demonstrates no DXR-induced change in PTEN protein expression levels, with or without Dexra pretreatment, at 4 h posttreatment.

inhibits DXR-induced follicle apoptosis signaling in marmoset ovarian tissue. Cleaved caspase-9 activates procaspase-3, leading to the formation of the apoptotic bodies [56]. Our data indicating a trend toward DXR-induced caspase 9 cleavage are consistent with previous studies demonstrating DXR activates caspase-3 in granulosa cells (which occurs downstream of caspase-9) and caspase-2 and -12 in oocytes in mice [57, 58]. Dexra-mediated attenuation of this DXR-induced trend in caspase-9 cleavage parallels our previous study in which pretreatment with Dexra prevented DXR-induced demise of immortalized murine granulosa cells assayed by cell cytotoxicity [34].

One proposed model for chemotherapy-induced ovarian insult has been termed the burn-out model [59]. The model describes enhanced primordial follicle activation due to depletion of growing follicles and subsequent primordial follicle growth and attrition, thus depleting the ovarian reserve [59]. Primordial follicle activation is initiated by oocyte growth and transition of granulosa cells from flat to cuboidal cells. Members of the PI3K signaling pathway, including AKT1 and PTEN, initiate primordial follicle activation [60]. To test the hypothesis that DXR treatment alters PI3K signaling, we examined AKT1 phosphorylation and PTEN expression. DXR appeared to activate AKT1 in marmoset ovarian slices, while Dexra maintained phosphorylated AKT1 at baseline control values. PTEN protein levels on the other hand did not change with DXR treatment in marmoset ovarian tissue culture at the time points tested; hence, restoration of PTEN by Dexra administration could not be tested in our model. PTEN is expressed specifically in oocytes, whereas AKT1 is expressed in granulosa cells. Depletion of PTEN from oocytes results in hyperactivation of AKT1, which in turn leads to rapid depletion of the primordial follicle pool [60]. The trend of DXR-induced AKT1 activation observed in the present study appeared independent of PTEN depletion, but is consistent with chemotherapy-induced premature ovarian failure. Future studies may assess the relationship between these cell division regulator proteins and both primordial follicle activation and ovarian cell survival following DXR insult.

Recently, there have been some concerns about the use of high-dose Dexra (Dexra:DXR 10:1 mg ratio) therapy for cardiac protection because of the possible association between high-dose Dexra and increased secondary blood cancers in children [61] and the suggestion that high-dose Dexra might diminish the anticancer efficacy of DXR in breast cancer patients [62]. The potential risk concerns raised by Tebbi et al. [61] did not reach statistical significance, and the slowed tumor response rate observed by Swain et al. [62] did not alter remission rate or patient survival. The majority of studies point toward an absence of pathogenic concern regarding Dexra, including a recent Cochrane review and other studies [63–65]. Nevertheless, the use of Dexra to provide skin and cardiac protection has been greatly restricted by the FDA to cancer patients receiving high doses of DXR ($\geq$300 mg/m^2) [66]. To mitigate the risk for complications following Dexra treatment, the current study utilized Dexra in a 1:1 mg ratio with DXR, rather than the 10:1 mg ratio currently utilized clinically [34, 67]. Administering Dexra at a dose tenfold lower than that used for cardioprotection appears to successfully protect somatic ovarian cells from acute DXR damage. Future studies are needed to confirm the long-term efficacy and safety profile of low-dose Dexra therapy in vivo prior to clinical use.

Taken together, the results from this study suggest that Dexra protects against acute DXR toxicity in marmoset ovarian tissue, preventing DNA damage, possibly through inhibition of apoptotic signaling. Our findings are limited by the low numbers of the animals tested because of the limited availability of marmoset ovarian tissue. These findings nevertheless support the use of the marmoset as a nonhuman primate for modeling ovarian toxicity and fertility preservation studies. This monkey is particularly suited for fertility studies given its relatively short generation time [40, 68]. These results are also encouraging for future translation of ovoprotection to an in vivo marmoset model to allow systematic assessment of the whole ovary for DXR toxicity and to assess the promise of low-dose Dexra protection.

ACKNOWLEDGMENT

The authors are very grateful to Dr. Mary Zeliniski for immense guidance and discussion and for providing ovarian tissue slicing protocols, Dr. Jon Levine for providing marmoset ovarian tissue for the study, Dr. Thaddeus G. Golos for generous assistance with interpretation of ovarian tissue histology slides, and Kim Keen for technical support on the Nikon A1 Confocal in the WNPRC. The authors would like to thank the WNPRC Nonhuman Primate Biological Materials Distribution Core and WNPRC Pathology Unit for nonhuman primate tissue collections and the Scientific Protocol Implementation Unit for surgical support.

REFERENCES

1. Siris ES, Leventhal BG, Vaitukaitis JL. Effects of childhood leukemia and chemotherapy on puberty and reproductive function in girls. N Engl J Med 1976; 294:1143–1146.
2. Shanis D, Merideth M, Pulanic TK, Savani BN, Battiwalla M, Stratton P. Female long-term survivors after allogeneic hematopoietic stem cell transplantation: evaluation and management. Semin Hematol 2012; 49: 83–93.
3. van Kasteren YM, Schoemaker J. Premature ovarian failure: a systematic review on therapeutic interventions to restore ovarian function and achieve pregnancy. Hum Reprod Update 1999; 5:483–492.
4. Salih SM, Elsarrag, SZ, Prange. E, Contreras. K, Osman. RG, Eikoff. J, Puccetti. D. Evidence to incorporate inclusive reproductive health measures in guidelines for childhood and adolescent cancer survivors. J Pediatr Adolesc Gynecol in press. Published online ahead of print 7 June 2014 as DOI: http://dx.doi.org/10.1016/j.jpag.2014.05.012.
5. Ethics Committee of American Society for Reproductive Medicine. Fertility preservation and reproduction in patients facing gonadotoxic therapies: a committee opinion. Fertil Steril 2013; 100:1224–1231.
6. Kucuk M. Fertility preservation for women with malignant diseases: ethical aspects and risks. Gynecol Endocrinol 2012; 28:937–940.
7. Bagchi A, Woods EJ, Critser JK. Cryopreservation and vitrification: recent advances in fertility preservation technologies. Expert Rev Med Devices 2008; 5:359–370.
8. Bromer JG, Patrizio P. Fertility preservation: the rationale for cryopreservation of the whole ovary. Semin Reprod Med 2009; 27:465–471.
9. Cao Y-X, Chian R-C. Fertility preservation with immature and in vitro matured oocytes. Semin Reprod Med 2009; 27:456–464.
10. Donnez J. Advances in fertility preservation for children and adolescents with cancer. Eur J Cancer 2009; 45(Suppl 1):418.
11. Ata B, Chian R-C, Tan SL, Dodds JE. Cryopreservation of oocytes and embryos for fertility preservation for female cancer patients. Best Pract Res Clin Obstet Gynaecol 2010; 24:101–112.
12. Behringer K, Wildt L, Mueller H, Mattle V, Ganitis P, van den Hoonaard B, Ott HW, Hofer S, Pluetschow A, Diehl V, Engert A, Borchmann P, et al. No protection of the ovarian follicle pool with the use of GnRH-analogues or oral contraceptives in young women treated with escalated BEACOPP for advanced-stage Hodgkin lymphoma. Final results of a phase II trial from the German Hodgkin Study Group. Ann Oncol 2010; 21:2052–2060.
13. Bedoschi G, Turan V, Oktay K. Utility of GnRH-agonists for fertility preservation in women with operable breast cancer: is it protective? Curr Breast Cancer Rep 2013; 5:302–308.
14. Oktay K, Sonmezer M. Gonadotropin-releasing hormone analogs in fertility preservation-lack of biological basis? Nat Clin Pract Endocrinol Metab 2008; 4:488–489.
15. Blumenfeld Z, Avivi I, Eckman A, Epelbaum R, Rowe JM, Dann EJ. Gonadotropin-releasing hormone agonist decreases chemotherapy-induced gonadotoxicity and premature ovarian failure in young female patients with Hodgkin lymphoma. Fertil Steril 2008; 89:166–173.
16. Zelinski MB, Murphy MK, Lawson MS, Jurisicova A, Pau KY, Toscano NP, Jacob DS, Fanton JK, Casper RF, Dertinger SD, Tilly JL. In vivo delivery of FTY720 prevents radiation-induced ovarian failure and infertility in adult female nonhuman primates. Fertil Steril 2011; 95:1440–1445.
17. Aubert N, Vaudry D, Falluel-Morel A, Desfeux A, Fisch C, Ancian P, de Jouffrey S, Le Bigot JF, Couvineau A, Laburthe M, Fournier A, Laudenbach V, et al. PACAP prevents toxicity induced by cisplatin in rat and primate neurons but not in proliferating ovary cells: involvement of the mitochondrial apoptotic pathway. Neurobiol Dis 2008; 32:66–80.
18. Ataya K, Rao LV, Lawrence E, Kimmel R. Luteinizing hormone-releasing hormone agonist inhibits cyclophosphamide-induced ovarian follicular depletion in rhesus monkeys. Biol Reprod 1995; 52:365–372.
19. Davis VJ. Female gamete preservation. Cancer 2006; 107:1690–1694.
20. Roti Roti EC, Leisman SK, Abbott DH, Salih SM. Acute doxorubicin

insult in the mouse ovary is cell- and follicle-type dependent. PLoS One 2012; 7:e42293.
21. Morita Y, Perez GI, Paris F, Miranda SR, Ehleiter D, Haimovitz-Friedman A, Fuks Z, Xie Z, Reed JC, Schuchman EH, Kolesnick RN, Tilly JL. Oocyte apoptosis is suppressed by disruption of the acid sphingomyelinase gene or by sphingosine-1-phosphate therapy. Nat Med 2000; 6: 1109–1114.
22. Paris F, Perez GI, Fuks Z, Haimovitz-Friedman A, Nguyen H, Bose M, Ilagan A, Hunt PA, Morgan WF, Tilly JL, Kolesnick R. Sphingosine 1-phosphate preserves fertility in irradiated female mice without propagating genomic damage in offspring. Nat Med 2002; 8:901–902.
23. Skaznik-Wikiel ME, McGuire MM, Sukhwani M, Donohue J, Chu T, Krivak TC, Rajkovic A, Orwig KE. Granulocyte colony-stimulating factor with or without stem cell factor extends time to premature ovarian insufficiency in female mice treated with alkylating chemotherapy. Fertil Steril 2013; 99:2045–2054.
24. Ting AY, Petroff BK. Tamoxifen decreases ovarian follicular loss from experimental toxicant DMBA and chemotherapy agents cyclophosphamide and doxorubicin in the rat. J Assist Reprod Genet 2010; 27:591–597.
25. Gonfloni S, Di Tella L, Caldarola S, Cannata SM, Klinger FG, Di Bartolomeo C, Mattei M, Candi E, De Felici M, Melino G, Cesareni G. Inhibition of the c-Abl-TAp63 pathway protects mouse oocytes from chemotherapy-induced death. Nature Medicine 2009; 15:1179–1185.
26. Kalich-Philosoph L, Roness H, Carmely A, Fishel-Bartal M, Ligumsky H, Paglin S, Wolf I, Kanety H, Sredni B, Meirow D. Cyclophosphamide triggers follicle activation and ''burnout''; AS101 prevents follicle loss and preserves fertility. Sci Transl Med 2013; 5:185ra62.
27. Roti Roti EC, Ringelstetter AK, Kropp J, Abbott DH, Salih SM. Bortezomib prevents acute doxorubicin ovarian insult and follicle demise, improving the fertility window and pup birth weight in mice. PLoS One 2014; 9:e108174.
28. Smith MA, Freidlin B, Ries LA, Simon R. Trends in reported incidence of primary malignant brain tumors in children in the United States. J Natl Cancer Inst 1998; 90:1269–1277.
29. Cancer in Children and Adolescents [Internet]. National Cancer Institute at NIH. http://www.cancer.gov/cancertopics/factsheet/Sites-Types/childhood. Accessed 20 December 2014.
30. Ben-Aharon I, Bar-Joseph H, Tzarfaty G, Kuchinsky L, Rizel S, Stemmer SM, Shalgi R. Doxorubicin-induced ovarian toxicity. Reprod Biol Endocrinol 2010; 8:20.
31. Bonilla E, del Mazo J. Deregulation of gene expression in fetal oocytes exposed to doxorubicin. Biochem Pharmacol 2003; 65:1701–1707.
32. Soleimani R, Heytens E, Darzynkiewicz Z, Oktay K. Mechanisms of chemotherapy-induced human ovarian aging: double strand DNA breaks and microvascular compromise. Aging 2011; 3:782–793.
33. Morita Y, Perez GI, Maravei DV, Tilly KI, Tilly JL. Targeted expression of Bcl-2 in mouse oocytes inhibits ovarian follicle atresia and prevents spontaneous and chemotherapy-induced oocyte apoptosis in vitro. Mol Endocrinol 1999; 13:841–850.
34. Roti Roti EC, Salih SM. Dexrazoxane ameliorates doxorubicin-induced injury in mouse ovarian cells. Biol Reprod 2012; 86:96.
35. Kane RC, McGuinn WD Jr, Dagher R, Justice R, Pazdur R. Dexrazoxane (Totect): FDA review and approval for the treatment of accidental extravasation following intravenous anthracycline chemotherapy. Oncologist 2008; 13:445–450.
36. Marty M, Espie M, Llombart A, Monnier A, Rapoport BL, Stahalova V. Multicenter randomized phase III study of the cardioprotective effect of dexrazoxane (Cardioxane) in advanced/metastatic breast cancer patients treated with anthracycline-based chemotherapy. Ann Oncol 2006; 17: 614–622.
37. Testore F, Milanese S, Ceste M, de Conciliis E, Parello G, Lanfranco C, Manfredi R, Ferrero G, Simoni C, Miglietta L, Ferro S, Giaretto L, et al. Cardioprotective effect of dexrazoxane in patients with breast cancer treated with anthracyclines in adjuvant setting: a 10-year single institution experience. Am J Cardiovasc Drugs 2008; 8:257–263.
38. Langer SW, Sehested M, Jensen PB, Buter J, Giaccone G. Dexrazoxane in anthracycline extravasation. J Clin Oncol 2000; 18:3064.
39. Martignoni M, Groothuis GM, de Kanter R. Species differences between mouse, rat, dog, monkey and human CYP-mediated drug metabolism, inhibition and induction. Expert Opin Drug Metab Toxicol 2006; 2: 875–894.
40. 't Hart BA, Abbott DH, Nakamura K, Fuchs E. The marmoset monkey: a multi-purpose preclinical and translational model of human biology and disease. Drug Discov Today 2012; 17:1160–1165.
41. von Schonfeldt V, Chandolia R, Kiesel L, Nieschlag E, Schlatt S, Sonntag B. Advanced follicle development in xenografted prepubertal ovarian tissue: the common marmoset as a nonhuman primate model for ovarian tissue transplantation. Fertil Steril 2011; 95:1428–1434.
42. Saltzman W, Digby LJ, Abbott DH. Reproductive skew in female common marmosets: what can proximate mechanisms tell us about ultimate causes? Proc Biol Sci 2009; 276:389–399.
43. Abbott DH, Barnett DK, Colman RJ, Yamamoto ME, Schultz-Darken NJ. Aspects of common marmoset basic biology and life history important for biomedical research. Comp Med 2003; 53:339–350.
44. Nubbemeyer R, Heistermann M, Oerke AK, Hodges JK. Reproductive efficiency in the common marmoset (Callithrix jacchus): a longitudinal study from ovulation to birth monitored by ultrasonography. J Med Primatol 1997; 26:139–146.
45. Gilchrist RB, Wicherek M, Heistermann M, Nayudu PL, Hodges JK. Changes in follicle-stimulating hormone and follicle populations during the ovarian cycle of the common marmoset. Biol Reprod 2001; 64:127–135.
46. Flaws JA, Abbud R, Mann RJ, Nilson JH, Hirshfield AN. Chronically elevated luteinizing hormone depletes primordial follicles in the mouse ovary. Biol Reprod 1997; 57:1233–1237.
47. Speth PA, van Hoesel QG, Haanen C. Clinical pharmacokinetics of doxorubicin. Clin Pharmacokinet 1988; 15:15–31.
48. Fraser HM, Hastings JM, Allan D, Morris KD, Rudge JS, Wiegand SJ. Inhibition of delta-like ligand 4 induces luteal hypervascularization followed by functional and structural luteolysis in the primate ovary. Endocrinology 2012; 153:1972–1983.
49. Li XH, Yang S, Lv XY, Sun HM, Weng J, Liang YJ, Zhou DS. The mechanism of mesna in protection from cisplatin-induced ovarian damage in female rats. J Gynecol Oncol 2013; 24:177–185.
50. Morgan S, Anderson RA, Gourley C, Wallace WH, Spears N. How do chemotherapeutic agents damage the ovary? Hum Reprod Update 2012; 18:525–535.
51. Kinner A, Wu WQ, Staudt C, Iliakis G. gamma-H2AX in recognition and signaling of DNA double-strand breaks in the context of chromatin. Nucleic Acids Res 2008; 36:5678–5694.
52. Mariotti LG, Pirovano G, Savage KI, Ghita M, Ottolenghi A, Prise KM, Schettino G. Use of the gamma-H2AX assay to investigate DNA repair dynamics following multiple radiation exposures. Plos One 2013; 8: e79541.
53. Novik KL, Spinelli JJ, Macarthur AC, Shumansky K, Sipahimalani P, Leach S, Lai A, Connors JM, Gascoyne RD, Gallagher RP, Brooks-Wilson AR. Genetic variation in H2AFX contributes to risk of non-Hodgkin lymphoma. Cancer Epidemiol Biomarkers Prev 2007; 16: 1098–1106.
54. Bassing CH, Suh H, Ferguson DO, Chua KF, Manis J, Eckersdorff M, Gleason M, Bronson R, Lee C, Alt FW. Histone H2AX: a dosage-dependent suppressor of oncogenic translocations and tumors. Cell 2003; 114:359–370.
55. Roos WP, Kaina B. DNA damage-induced cell death by apoptosis. Trends Mol Med 2006; 12:440–450.
56. Elmore S. Apoptosis: a review of programmed cell death. Toxicol Pathol 2007; 35:495–516.
57. Rebbaa A, Zheng X, Chou PM, Mirkin BL. Caspase inhibition switches doxorubicin-induced apoptosis to senescence. Oncogene 2003; 22: 2805–2811.
58. Takai Y, Matikainen T, Jurisicova A, Kim MR, Trbovich AM, Fujita E, Nakagawa T, Lemmers B, Flavell RA, Hakem R, Momoi T, Yuan J, et al. Caspase-12 compensates for lack of caspase-2 and caspase-3 in female germ cells. Apoptosis 2007; 12:791–800.
59. Roness H, Gavish Z, Cohen Y, Meirow D. Ovarian follicle burnout: a universal phenomenon? Cell Cycle 2013; 12:3245–3246.
60. Reddy P, Liu L, Adhikari D, Jagarlamudi K, Rajareddy S, Shen Y, Du C, Tang W, Hamalainen T, Peng SL, Lan ZJ, Cooney AJ, et al. Oocyte-specific deletion of Pten causes premature activation of the primordial follicle pool. Science 2008; 319:611–613.
61. Tebbi CK, London WB, Friedman D, Villaluna D, De Alarcon PA, Constine LS, Mendenhall NP, Sposto R, Chauvenet A, Schwartz CL. Dexrazoxane-associated risk for acute myeloid leukemia/myelodysplastic syndrome and other secondary malignancies in pediatric Hodgkin's disease. J Clin Oncol 2007; 25:493–500.
62. Swain SM, Whaley FS, Gerber MC, Ewer MS, Bianchine JR, Gams RA. Delayed administration of dexrazoxane provides cardioprotection for patients with advanced breast cancer treated with doxorubicin-containing therapy. J Clin Oncol 1997; 15:1333–1340.
63. van Dalen EC, Caron HN, Dickinson HO, Kremer LC. Cardioprotective interventions for cancer patients receiving anthracyclines. Cochrane Database Syst Rev 2011; (6):CD003917.
64. Vejpongsa P, Yeh ET. Prevention of anthracycline-induced cardiotoxicity: challenges and opportunities. J Am Coll Cardiol 2014; 64:938–945.

65. Vrooman LM, Neuberg DS, Stevenson KE, Asselin BL, Athale UH, Clavell L, Cole PD, Kelly KM, Larsen EC, Laverdiere C, Michon B, Schorin M, et al. The low incidence of secondary acute myelogenous leukaemia in children and adolescents treated with dexrazoxane for acute lymphoblastic leukaemia: a report from the Dana-Farber Cancer Institute ALL Consortium. Eur J Cancer 2011; 47:1373–1379.
66. FDA Statement on Dexrazoxane [Internet]. U.S. Food and Drug Administration. http://www.fda.gov/Drugs/DrugSafety/ucm263729.htm. Accessed: 20 December 2014.
67. Lipshultz SE, Scully RE, Lipsitz SR, Sallan SE, Silverman LB, Miller TL, Barry EV, Asselin BL, Athale U, Clavell LA, Larsen E, Moghrabi A, et al. Assessment of dexrazoxane as a cardioprotectant in doxorubicin-treated children with high-risk acute lymphoblastic leukaemia: long-term follow-up of a prospective, randomised, multicentre trial. Lancet Oncol 2010; 11: 950–961.
68. Orsi A, Rees D, Andreini I, Venturella S, Cinelli S, Oberto G. Overview of the marmoset as a model in nonclinical development of pharmaceutical products. Regul Toxicol Pharmacol 2011; 59:19–27.